One-pot fabrication of carboxyl-functionalized biocompatible magnetic nanocrystals for conjugation with targeting agents†

Chichong Lu,*[a] Zhe-Shan Quan,[b] Jung Chul Sur,[c] Sun-Hee Kim,[d] Choong Hun Lee[c] and Kyu Yun Chai*[a]

Received (in Montpellier, France) 26th January 2010, Accepted 28th April 2010
DOI: 10.1039/c0nj00067a

In this study, we prepared biocompatible, water-soluble, superparamagnetic, manganese-doped, magnetism-engineered iron oxide (MnMEIO) nanocrystals with reactive moieties. This was achieved *via* a one-pot synthesis protocol by thermally decomposing metal acetylacetonate precursors in 2-pyrrolidone in the presence of polyethylene glycol diacid. Using carbodiimide, we achieved nanocrystals coupled with 9-aminoacridine and folic acid through 2,2′-(ethylenedioxy)-bis-ethylamine. The results suggest that the nanocrystals provide carboxyl functional groups as binding sites. Their surface modification and composition were analyzed by Fourier transform infrared (FTIR) spectroscopy and X-ray photoelectron spectroscopy (XPS), respectively. Using Mössbauer spectroscopy and a magnetometer, we have shown that these nanocrystals exhibit superparamagnetic behaviors. In addition, we have demonstrated that the nanocrystals were not significantly toxic, and hence are biocompatible.

Introduction

There has been considerable interest in the development of a variety of functional nanometre-sized colloidal nanocrystals for their tunable magnetic properties, as well as for potential biomedical applications, including magnetic resonance imaging (MRI), cell and protein separation, and drug delivery.[1–4] Furthermore, cell-specific targeting and therapeutic agents can be incorporated into a single magnetic nanoparticle designed for the simultaneous diagnosis and treatment of diseased tissues. The recent development of molecular and cellular imaging to aid visualization of disease-specific biomarkers at the molecular and cellular levels has led to a growing interest in magnetic nanocrystals. An example of specific targeting ligands is folic acid (FA). FA has the ability to preferentially target cancer cells (in the ovaries, kidney, uterus, testes, brain, colon and lungs) because the folate receptor is frequently over-expressed on their surfaces.[5] Wiener and co-workers have reported that FA attached to polyamidoamine (PAMAM) increased the longitudinal relaxation rate in tumor cells with an excessive expression of the high-affinity folate receptor.[6] This new method for the treatment of tumors greatly enhances the scope of nanoparticle application. Therefore, the development of an efficient ligand conjugate system that targets magnetic nanocrystals is an eminent challenge in this field of research.

[a] *Department of Bionanochemistry, Wonkwang University, Iksan, Jeonbuk 570-749, South Korea. E-mail: geuyoon@wonkwang.ac.kr; Fax: +82 63 8414893; Tel: +82 63 8506230*
[b] *College of Pharmacy, Yanbian University, Yanji, Jilin 133000, P. R. China*
[c] *Division of Microelectronics and Display Technology, Wonkwang University, Iksan, Jeonbuk 570-749, South Korea*
[d] *Department of Nuclear Medicine, Chonbuk National University Medical School and Hospital, Jeonju, Jeonbuk 561-712, South Korea*
† Electronic supplementary information (ESI) available: EDX, UV-vis, stability test and MR images of MnMEIO nanocrystals. See DOI: 10.1039/c0nj00067a

Although magnetic nanocrystals have long been of scientific and technological interest, and have shown significant potential for many important biomedical applications, several requirements must be met before these nanocrystals can be successfully used *in vivo*. These include good dispersibility in physiological media, biocompatibility and the ability to resist phagocytosis by the reticuloendothelial system (RES) to the uptake of magnetic nanocrystals. Therefore, surface complexing agents such as dextran, polyethylene glycol (PEG) and small ligand molecules are often used to provide colloid stability and biocompatibility.[7–10]

The recently developed thermal decomposition method has been demonstrated to be an effective approach for synthesizing high-quality magnetic nanocrystals. Sun *et al*. have reported the synthesis of monodispersed MFe_2O_4 (M = Fe, Mn, Co) nanoparticles using $Fe(acac)_3$ as the starting material.[11] However, the direct products of the above-mentioned approaches are insoluble in aqueous media, which, to some extent, limits their applications in biological fields. Zhang and co-workers modified these nanoparticles by appending a PEG-silane functional group using sophisticated post-preparative procedures and demonstrated the biocompatibility of the functionalized magnetite nanoparticles.[8] Gao *et al*. have established a synthetic method for preparing PEG-coated Fe_3O_4 nanocrystals *via* a one-pot reaction in strongly polar 2-pyrrolidone. These water-soluble and biocompatible magnetite nanocrystals were demonstrated to be useful for disease detection in either passive or active modes.[12–14] These observations point toward the possibility of synthesizing suitably-derived, biofunctionalized, manganese-doped, magnetism-engineered iron oxide (MnMEIO) nanocrystals *via* a one-pot reaction, owing to their better sensitivity in biomedical applications, the ease with which their surface can be modified and their higher magnetic moment compared to that of other conventional iron oxide-based magnetic nanocrystals.[15–17]

Here, in order to prepare water-soluble, multifunctional magnetic nanocrystals, we report a novel one-pot reaction approach for synthesizing Mn-doped Fe_3O_4 nanocrystals, 12 and 27 nm in size and covalently coated by polyethylene glycol diacid (HOOC–PEG–COOH). Using carbodiimide, these nanocrystals functionalized with carboxyl groups were then coupled with 9-aminoacridine and FA through 2,2′-(ethylenedioxy)-bis-ethylamine, a hydrophilic linker. The nanocrystals were characterized and confirmed by TEM, FTIR, XRD, XPS, EDX and UV-vis spectroscopy. Using Mössbauer spectroscopy and a magnetometer, we have shown that these nanocrystals exhibit superparamagnetic behaviors. In addition, the nanocrystals were examined by a 3-(4,5-dimethylthiazol-2-yl)-2,5-diphenyltetrazolium bromide (MTT) assay to demonstrate that they have no significant toxicity, and hence are biocompatible.

Experimental

Materials

The following materials were purchased from Sigma-Aldrich and were used as received: 2,2′-(ethylenedioxy)-bis-ethylamine (EDBE), 1-ethyl-3-(3-dimethylaminopropyl) carbodiimide hydrochloride (EDC), *N*-hydroxysuccinimide (98%; NHS), iron(III) acetylacetonate, manganese(II) acetylacetonate and 9-aminoacridine hydrochloride hydrate (98%; 9-AA). FA was purchased from Acros Organics. 2,2,6,6-Tetramethylpiperidine-1-oxyl (TEMPO), a free radical, was purchased from Tokyo Chemical Industry.

Synthesis of carboxyl Mn-doped Fe_3O_4 nanocrystals

Polyethylene glycol diacids (HOOC–PEG–COOH) having different molecular weights were prepared by reported experimental methods using TEMPO as a catalyst at 57 °C for 24 h.[12] Biocompatible and water-soluble carboxyl MnMEIO nanocrystals were synthesized by the thermal decomposition method using strongly polar 2-pyrrolidone as a coordinating solvent, and covalently modifying the MnMEIO nanocrystals with PEG diacid *via* its carboxyl group. 12 nm carboxyl MnMEIO nanocrystals were synthesized as follows: A solution of 20 mL of purified 2-pyrrolidone containing 0.353 g $Fe(acac)_3$, 0.063 g $Mn(acac)_2$ and 2.2 g polyethylene glycol diacid (M_n = 2000) was prepared. After being purged with nitrogen for 30 min to remove oxygen, the reaction mixture was pre-heated at 200 °C for 30 min and refluxed at 240 °C for 1.5 h. Subsequently, the resulting mixture was cooled to room temperature and 100 mL of an ether/acetone mixture (5 : 1) added to the mixture to precipitate the resultant nanocrystals. The black precipitate was washed several times with ether/acetone (5 : 1) and then dried. 27 nm biocompatible carboxyl MnMEIO nanocrystals were synthesized in a similar fashion using pre-selected reaction parameters. In a three-necked flask, 0.706 g $Fe(acac)_3$, 0.126 g $Mn(acac)_2$ and 5.1 g polyethylene glycol diacid (M_n = 3400) were dissolved in 20 mL of 2-pyrrolidone. After being purged with nitrogen for 30 min, the reaction solution was refluxed for 10 h. Subsequently, carboxyl-functionalized biocompatible MnMEIO nanocrystals were obtained after a set of post-processing procedures that were the same as those for the 12 nm nanocrystals.

Surface modification of Mn-doped Fe_3O_4 nanocrystals

9-Aminocaridine (9-AA) was attached to the nanocrystal surface by coupling the amine group of 9-AA to the carboxyl group of the PEG-coated nanocrystals using NHS/EDC (*N*-hydroxysuccinamide, 1-ethyl-3-(3-dimethylaminopropyl) carbodiimide) covalent chemistry. The process used for achieving this was an improvisation of previously described methods.[13] 2 mg EDC and 3 mg NHS were added to a 15 mL aqueous solution of the nanocrystals (1 mg MnMEIO mL^{-1}). After approximately 15 min, a 0.3 mL acetone solution containing 0.7 mg 9-AA was introduced, and the pH of the reaction system adjusted to 7.5 by adding 1 M NaOH. The reactants were stirred overnight at room temperature (R.T.), and then an acetone/ether mixture (5 : 1) was added to precipitate the resulting 9-AA-conjugated nanocrystals. After being washed several times with an acetone/ether mixture (1 : 1) until no fluorescence was detected from the supernatant, the resulting 9-AA-conjugated nanocrystals were dried *in vacuo*.

To conjugate the nanocrystals with FA, EDBE was used as a starting material for the synthesis of amino-modified FA ($FA\text{-}NH_2$).[18,19] The nanocrystals were dissolved in 50 mL of de-ionized water along with 90 mg of NHS and 750 mg of EDC. The solution was stirred for 4 h, following which the nanocrystals were isolated and resuspended in 50 mL of DMSO, along with 97 mg of $FA\text{-}NH_2$. The resulting suspension was agitated overnight at 37 °C in the absence of light. Following FA conjugation, the modified nanocrystals were centrifuged, washed three times with de-ionized water and then stored in de-ionized water.

In vitro cell viability

To determine the cytotoxicity of conjugated MnMEIO nanocrystals, mouse macrophage cells (RAW 264.7) were seeded into 96-well plates for 24 h at densities of 1×10^4 cells per well at 37 °C in a 5% CO_2 atmosphere. Magnetic nanocrystals at final concentrations of 50, 100, 150 and 200 μg mL^{-1} were added to the cells and incubated for 48 h. The cells were washed twice with PBS and replenished with fresh medium. Subsequently, the cells were examined with an MTT assay.

Characterization

^1H and ^{13}C NMR spectra were measured using a JEOL FT/NMR spectrometer. IR spectra were acquired using a Shimadzu IRPrestige-21 FTIR spectrometer with a resolution of 4 cm^{-1}. Samples of the surface-modified nanocrystals were dried overnight using a freeze-drier. Then, the nanocrystals were milled with KBr and the mixture pressed into a pellet for analysis. Powder X-ray diffraction (XRD) patterns were acquired from the dried nanocrystal samples by a Rigaku powder X-ray diffractometer using Cu-K_α radiation (λ = 1.541 Å) at 40 kV and 30 mA. Transmission electron microscopy (TEM) images were acquired on a Hitachi H7650 Bio-TEM instrument operating at 100 kV. All UV-vis absorbance experiments were conducted on Shimadzu UV-2450 spectrophotometers with water circulated cell blocks. A quartz cell

with a 1 cm path length was used for all of the absorbance studies. The surface compositions of the nanocrystals were obtained by analyzing X-ray photoelectron spectroscopy (XPS) and a laboratory-based spectrometer (K-alpha, Thermo.) using a photon energy of 1486.6 eV (Al-K_α). Energy dispersive X-ray spectroscopy (EDX) was undertaken on a Hitachi FE-SEM equipped with an EDX detector (Horiba). ^{57}Co electromechanical-type Mössbauer spectroscopy was carried out in sinusoidal mode. The magnetic properties were measured by means of a superconducting quantum interference device (SQUID, Quantum Design MPMS XL7) magnetometer.

Results and discussion

Magnetic nanocrystals have shown great potential in biomedical applications, particularly in the introduction of ferromagnetic or superparamagnetic particles into tumor tissue.[20] However, the major drawback impeding the further biological application of nanocrystals with superior properties has been the fact that synthetic approaches have yielded nanocrystals that are insoluble in aqueous media. Recently, an alternative method was developed to synthesize high quality magnetic nanocrystals by a thermal decomposition method. Here, we have chosen manganese-doped, magnetism-engineered iron oxide nanocrystals as a model system for bio-functionalization, immobilization and detection. MnMEIO has a very low magnetocrystalline anisotropy and a high magnetic moment compared to other high-moment ferrites, *i.e.*, γ-Fe_2O_3, Fe_3O_4 and $CoFe_2O_4$.[15–17] Biocompatible and water-soluble carboxyl MnMEIO nanocrystals with reactive moieties were prepared *via* a one-pot synthesis protocol involving the thermal decomposition of metal acetylacetonate precursors using strongly polar 2-pyrrolidone as a coordinating solvent and covalently modifying the nanocrystals with PEG diacid *via* its carboxyl group. Derivatives of PEG that undergo easy formation of an organic layer on the surface of nanocrystals are useful for introducing functional groups on the surface of magnetic nanocrystals. These PEG layers render the nanocrystals stable with respect to aggregation, keeping them well-dispersed in aqueous media, such that their anti-biofouling properties improve their intracellular uptake.

Fig. 1 presents representative transmission electron microscopy (TEM) images of MnMEIO nanocrystals with average diameters of 12 and 27 nm (see ESI, Fig. S1†). The X-ray diffraction (XRD) patterns for the 12 nm undoped and Mn-doped Fe_3O_4 nanocrystals are presented in Fig. 2. Although the nanocrystals were covered with organic components, it was observed from the XRD patterns that all of the peaks in both the undoped and Mn-doped magnetism-engineered iron oxide nanocrystals could be assigned to the inverse cubic spinel structure of magnetite. This indicates that the crystal structure of the Mn-doped nanocrystals is similar to that of magnetite. Moreover, a crystal orientation corresponding to Mn was not detected in any of the doped nanocrystals. Consequently, it is considered that MnMEIO nanocrystals could be fabricated by a one-pot reaction approach.

In order to confirm the Mn present and the surface modification, the nanocrystals were authenticated using XPS

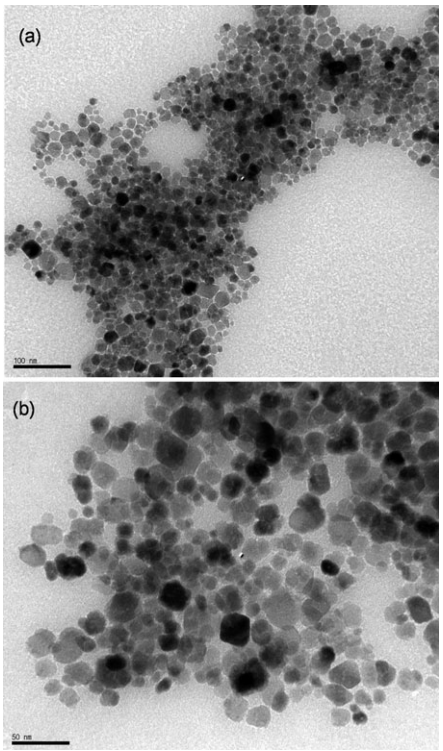

Fig. 1 TEM images of (a) 12 nm and (b) 27 nm MnMEIO nanocrystals. The scale bar corresponds to (a) 100 nm and (b) 50 nm.

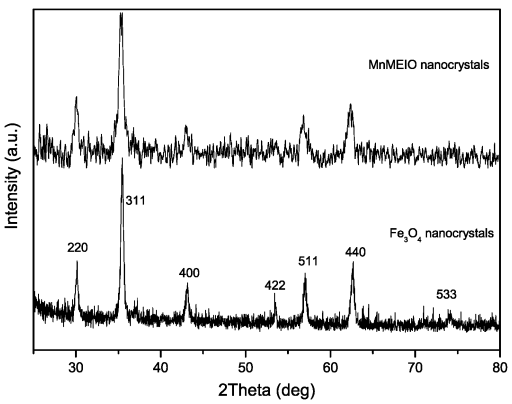

Fig. 2 X-ray diffraction patterns of the 12 nm Mn-doped and undoped Fe_3O_4 nanocrystals.

measurements. The topical survey spectrum of 12 nm MnMEIO is presented in Fig. 3. The high resolution C 1s spectrum displays a broad shoulder in-between 280 and 292 eV. Taking bulk C 1s at 285 eV as standard, the broad shoulder can be fitted into two peaks at 285.1 and 286.6 eV, which can be attributed to C–C and C–O groups, respectively. The O 1s spectrum displays two peaks at 532.5 and 530.3 eV, corresponding to oxygen being present in two different environments: C–O and metal oxide. The broad peak for N 1s could be fitted into two peaks at 398.6 and 400.3 eV, corresponding to N–H and C–N within the 2-pyrrolidone structure on the surface of the magnetic nanocrystals. The binding energies of Fe $2p_{3/2}$ and Fe $2p_{1/2}$ appear at 710 and 724 eV, corresponding to Fe–O bonds, which are typical of

core level spectra of Fe_3O_4.[21,22] The Mn 2p doublet with binding energy values of 641 and 652 eV implies the presence of Mn–O bonds. The Mn content is estimated to be about 12% from the integration of the Fe and Mn peaks. The EDX data of the 12 nm MnMEIO is shown in the ESI, Fig. S2.† Mn substitution takes place over the entire nanocrystal with an average content ([Mn]/([Fe] + [Mn]) of 0.1, which is close to that determined from the XPS data.

To study the magnetic behavior of the nanocrystals, we performed magnetization measurements using Mössbauer spectroscopy. Fig. 4 shows the Mössbauer spectra of the 12 nm Mn-doped magnetism-engineered iron oxide nanocrystals and Fe_3O_4 nanocrystals at room temperature. The Fe_3O_4 nanocrystals were prepared according to the procedure outlined in ref. 13. The absorption lines consisted of a sextet and a doublet. Essentially, the spectra were composed of contributions from two different magnetic states. The doublet line indicates the superparamagnetic state of the sample and the sextet line indicates the ferromagnetic state. The proportions of the superparamagnetic and ferromagnetic states in the 12 nm magnetite nanocrystals were calculated from absorption line areas as being 27 and 73%, respectively, whereas, the 12 nm Mn-doped Fe_3O_4 nanocrystals exhibited exclusively superparamagnetic behaviors. The broad sextet in the magnetite nanocrystals showed particles of almost superparamagnetic size. In addition, the 27 nm magnetic Mn-doped Fe_3O_4 nanocrystals and the Fe_3O_4 nanocrystals showed different magnetic states (Fig. 4). This demonstrates that the 27 nm Fe_3O_4 nanocrystals are ferromagnetic, while the 27 nm Mn-doped Fe_3O_4 nanocrystals simultaneously exhibit superparamagnetic and ferromagnetic states at room temperature. The 27 nm Fe_3O_4 nanocrystals were 100% magnetically ordered; however, this decreased to 80% for the 27 nm Mn-doped Fe_3O_4 nanocrystals. It is inferred from the Mössbauer studies that the Mn-doped Fe_3O_4 nanocrystals exhibited a unique superparamagnetic behavior in the 12 nm Mn-doped Fe_3O_4 nanocrystals. This ensures the application of Mn-doped Fe_3O_4 nanocrystals in biomedical and bioengineering fields as they do not retain any magnetism after the removal of a magnetic field.

The magnetization *vs.* magnetic field (M–H) curves obtained at room temperature for both the 12 and 27 nm magnetic crystals are illustrated in Fig. 5. Our results show that the 12 nm MnMEIO nanocrystals exhibit superparamagnetic behavior without magnetic hysteresis, while the 27 nm nanocrystals are ferrimagnetic. The saturation magnetization of the samples was found to be 51 and 74 emu g^{-1}, respectively. As is evident, the M_s value of both MnMEIO nanocrystal types is

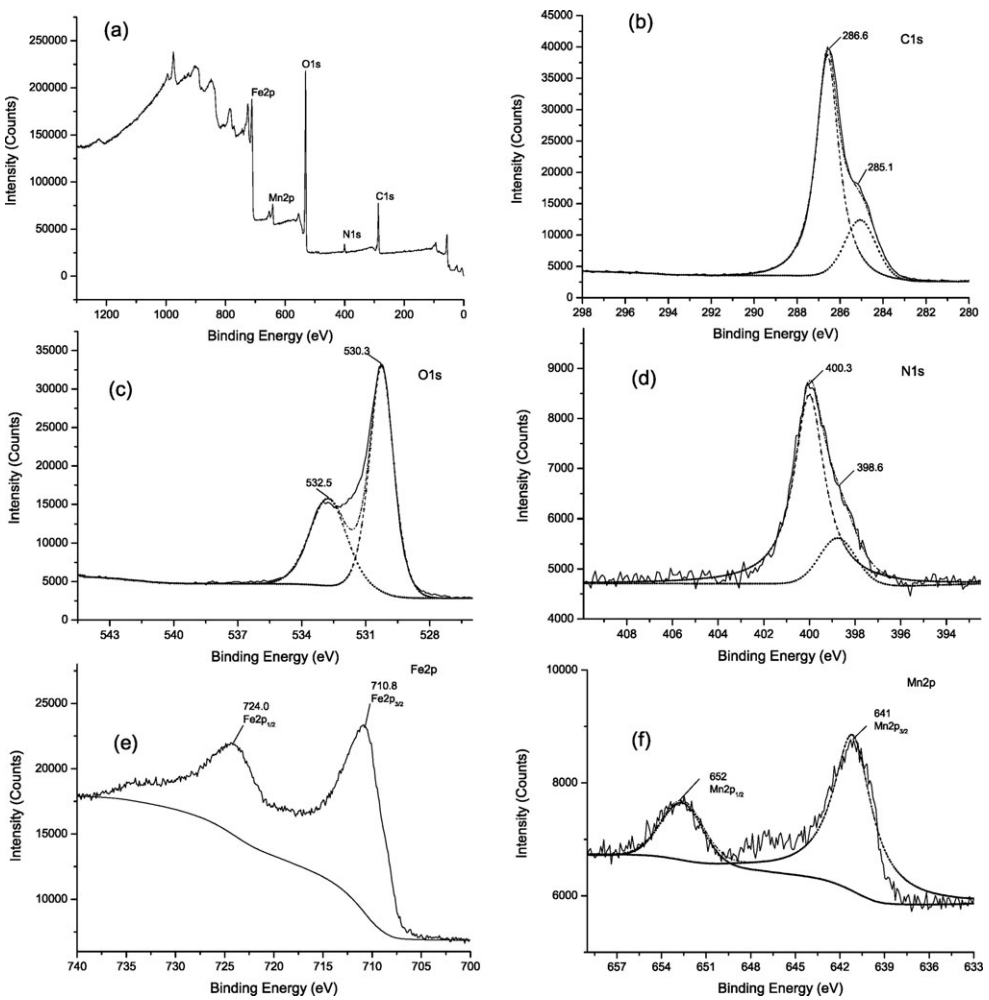

Fig. 3 XPS spectra of 12 nm MnMEIO nanocrystals presenting (a) a survey, and (b) C1s, (c) O1s, (d) N1s, (e) Fe2p and (f) Mn2p spectra.

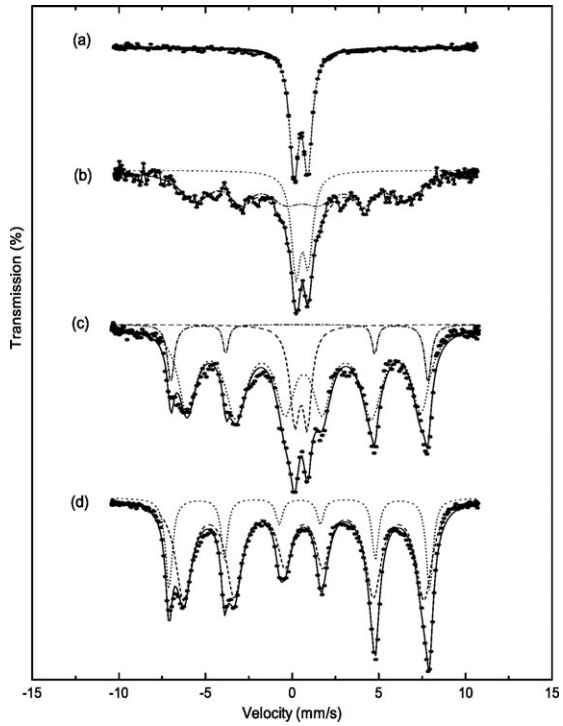

Fig. 4 Mössbauer spectra at room temperature for the (a) 12 nm Mn-doped and (b) undoped Fe_3O_4 nanocrystals, and (c) 27 nm Mn-doped and (d) undoped Fe_3O_4 nanocrystals.

larger than that of the magnetite nanocrystals.[13] The difference in the M_s value of our samples should be mainly contributed to by the differences in particle size and partially contributed to by the diamagnetic organic coating.

The better sensitivity of MnMEIO than Fe_3O_4 in MRI applications has recently been demonstrated for individual nanoparticles.[15] To evaluate the effectiveness of the nanocrystals as MRI agents, the 12 nm MnMEIO and Fe_3O_4 nanocrystals were diluted in test tubes to different concentrations. In the T_2-weighted MR images at 1.5 T, MR contrasts were strong and became more intense with increasing amounts of the nanocrystals (ESI, Fig. S3†), and the 12 nm MnMEIO nanocrystals exhibited a much stronger enhancement in both

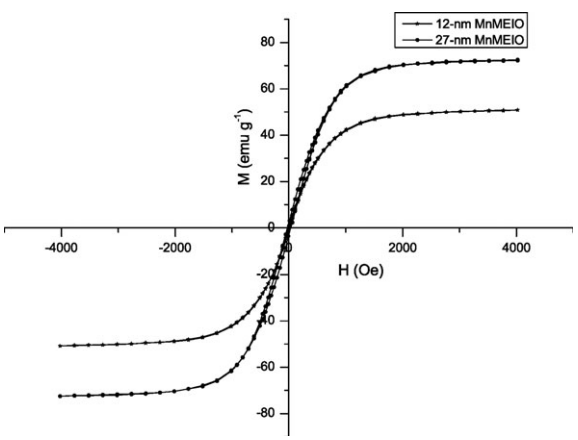

Fig. 5 Magnetization curves of 12 and 27 nm MnMEIO nanocrystals at room temperature.

T_1- and T_2-weighted MRI than the Fe_3O_4 nanocrystals. The results of the MRI study clearly show that the MnMEIO nanocrystals exhibited the stronger susceptibility effect.

These superparamagnetic nanocrystals provide the free carboxyl groups that can be used to immobilize other molecules in aqueous media. To demonstrate this, we designed 9-AA and FA to attach to the nanocrystals' surface. 9-AA has been proposed as a specific fluorescent probe in the position to bind the active center of certain enzymes and nucleic acids, including guanidinobenzoatases (GB). Here, it was immobilized on the nanocrystal surface not only as a fluorescent probe, but also as an antibacterial, mutagenic and anticancer drug due to its interaction with DNA. These enzymes have proteolytic activity associated with the development of tumoral processes and neoplastic metastasis. In fact, the staining of 9-AA in histopathological sections has been used to locate malignant cells in many tumor tissues.[23] The 9-AA successfully grafted onto the surface of nanocrystals was analyzed and confirmed by Fourier transform infrared (FTIR) spectroscopy. The FTIR spectra of the 12 nm MnMEIO nanocrystals are shown in Fig. 6, along with those of PEG. The C–O–C ether stretching band at 1103 cm^{-1} and the asymmetric stretching band at 1350 cm^{-1} appear in the FTIR spectra of both PEG and the magnetic nanocrystals. Similarly, the bands at 2923 and 2864 cm^{-1} correspond to the C–H asymmetric band and the C–H symmetric stretching band, respectively. The bands at 950 cm^{-1} correspond to –CH– out-of-plane bending vibrations.[24,25] These peaks are strong evidence that the nanocrystal surface is coated with PEG. The characteristic absorption peaks of 9-AA at 1658, 1637, 1591 and 1240 cm^{-1} were also observed in the spectrum of 9-AA-modified magnetic nanocrystals (Fig. 6), indicating that 9-AA was successfully immobilized on the nanocrystals' surface. In addition, a very broad absorption band of the conjugated nanocrystals above 3000 cm^{-1} is present in the spectra. This may be attributed to the overlap of the N–H stretching band at around 3115 cm^{-1} from 9-AA and the N–H stretching band at 3324 cm^{-1} from 2-pyrrolidone binding[13] on the surface of the magnetic nanocrystals.

The surface chemistry of the FA-conjugated nanocrystals was also characterized by FTIR spectroscopy. The FTIR spectrum of the FA standard presents characteristic bands at 1695 and 1606 cm^{-1}. The characteristic peaks of the biocompatible nanocrystals, as well as FA, appeared in the FTIR spectrum (Fig. 7), indicating that FA had been successfully grafted to the nanocrystals. FTIR spectrum (b) shows an increased absorbance at 1637 cm^{-1} and the appearance of a new band at around 1560 cm^{-1}, arising from the amide bands within the FA structure, as well as those between FA and the carboxyl-functionalized nanocrystals.[26,27] This further verifies the formation of an extra amide bond during the grafting of FA to the nanocrystals.

To further verify the successful synthesis of the 9-AA-attached nanocrystals, UV-vis absorption spectra were also obtained. The absorption spectrum of 9-AA, the magnetic nanocrystals and their conjugate is shown in Fig. S4.† The absorbance of 9-AA is roughly superimposed on that of the magnetic nanocrystals, revealing an enhanced absorbance for the conjugates.[13] On the other hand, both the carboxyl

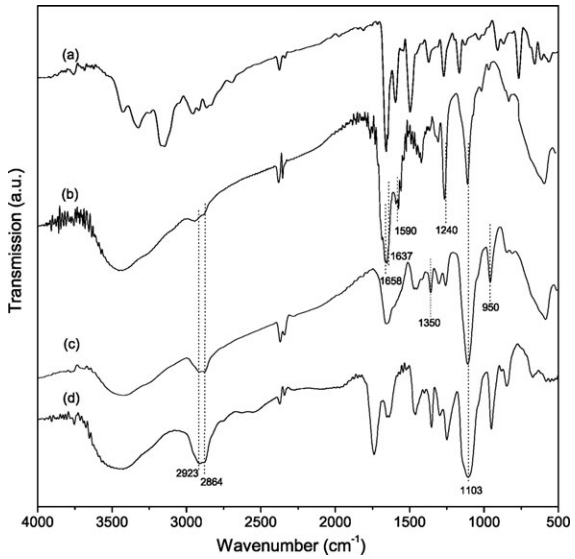

Fig. 6 FTIR spectra of (a) 9-AA, (b) 9AA-conjugated nanocrystals, (c) the 12 nm MnMEIO nanocrystals and (d) PEG diacid (M_n = 2000).

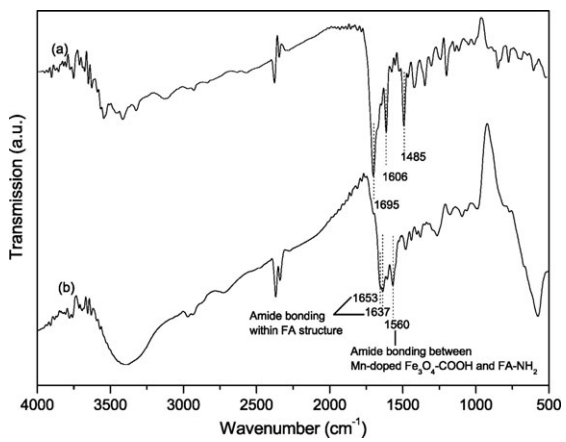

Fig. 7 FTIR spectra of (a) FA and (b) the FA-grafted nanocrystals.

nanocrystals and the FA-grafted nanocrystals well dispersed in phosphate-buffered saline (pH 7.4) were stable for up to a month under ambient conditions without any sign of aggregation (ESI, Fig. S4†).

In order to provide a more quantitative comprehension of the magnetic nanocrystals, the nitrogen and carbon composition in wt% of the 12 nm MnMEIO nanocrystals and the 9-AA-conjugated nanocrystals were obtained by elemental analysis (ESI, Table S1†). The molar ratio of 2-pyrrolidone to PEG was calculated to be about 6.8, approximately the same as for the magnetite nanocrystals. Assuming that the density of the MnMEIO nanocrystals is same as that of bulk magnetite (5.24 g cm^{-3})[13,28] and the number of surface molecules is identical to the number of magnetite structural units on the particle surface, the number of carboxyl groups on each 12 nm diameter spherical MnMEIO nanocrystal was estimated to be about 270, which is close to that estimated from the thermogravimetric analysis data (ESI,

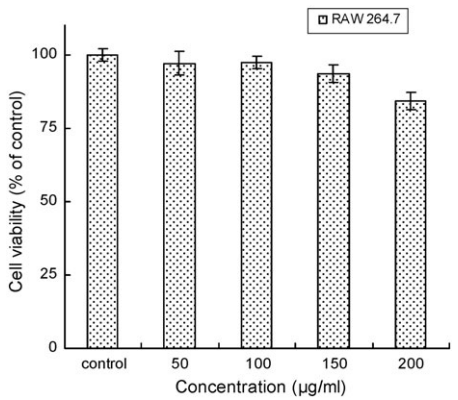

Fig. 8 The effect of 12 nm MnMEIO nanocrystals on the viability of RAW 264.7 cells. Cells were incubated with or without the nanocrystals for 48 h at 37 °C, followed by the MTT assay.

Fig. S5†). Furthermore, the molar ratio of 9-AA to PEG in the nanocrystals was calculated to be about 0.6 based on the elemental analysis. Therefore, this result suggests that the magnetic nanocrystals were modified, with a carboxyl functional group as the binding site.

An MTT assay using the RAW 264.7 cell line, which has been described as a suitable method for detection of biomaterial toxicity, was performed to analyze the potential toxicity of the magnetic nanocrystals.[29] Cells were incubated with various nanocrystal concentrations up to 200 μg mL^{-1} (Fig. 8). The results indicate that the nanocrystals showed no significant toxicity, even at relatively high concentrations (200 μg mL^{-1}), far exceeding that of iron used in conventional magnetite-based MR contrast agents for mice (1–20 mg kg^{-1}). The results suggest that the nanocrystals are safe, and as such could be potential candidates as MR imaging agents for *in vivo* applications.

Conclusions

In this study, biocompatible and water-soluble, superparamagnetic MnMEIO nanocrystals with reactive moieties were prepared *via* a one-pot synthesis protocol involving a thermal decomposition method. MnMEIO nanocrystals of different sizes could be obtained simply by varying the reaction parameters. In addition, the FA and 9-AA successfully grafted onto the nanocrystals' surface demonstrates that the nanocrystals provide the free carboxyl groups for immobilization of targeting ligands in aqueous media. We believe that this novel synthetic approach will pave a new way for the preparation of water-soluble, biocompatible MnMEIO nanocrystals, and that these nanocrystals could potentially be used for high quality nanoplatforms in MR imaging and drug delivery systems.

Acknowledgements

This work was supported by the Regional Innovation Center for Next Generation Industrial Radiation Technology at Wonkwang University (2009).

References

1 K. J. Klabunde, *Nanoscale Materials in Chemistry*, Wiley-Interscience, New York, 2001.
2 A. P. Alivisatos, *Science*, 1996, **271**, 933.
3 T. Hyeon, *Chem. Commun*., 2003, 927.
4 J. Park, J. Joo, S. G. Kwon, Y. Jang and T. Hyeon, *Angew. Chem., Int. Ed*., 2007, **46**, 4630.
5 S. D. Weitman, R. H. Lark, L. R. Coney, D. W. Fort, V. Frasca, V. R. Zurawski and B. A. Kamen, *Cancer Res*., 1992, **52**, 3396.
6 E. C. Wiener, S. Konda, A. Shadron, M. Brechbiel and O. Gansow, *Invest. Radiol*., 1997, **32**, 748.
7 J.-H. Park, G. Maltzahn, L. Zhang, M. P. Schwartz, E. Ruoslahti, S. N. Bhatia and M. J. Sailor, *Adv. Mater*., 2008, **20**, 1630.
8 N. Kohler, G. E. Fryxell and M. Zhang, *J. Am. Chem. Soc*., 2004, **126**, 7206.
9 (*a*) A. G. Kanaras, F. S. Kamounah, K. Schaumburg, C. J. Kiely and M. Brust, *Chem. Commun*., 2002, 2294.
10 S. Wagner, J. Schnorr, H. Pilgrimm, B. Hamm and M. Taupitz, *Invest. Radiol*., 2002, **37**, 167.
11 S. Sun, H. Zeng, D. B. Robinson, S. Raoux, P. M. Rice, S. X. Wang and G. Li, *J. Am. Chem. Soc*., 2004, **126**, 273.
12 Z. Li, L. Wei, M. Gao and H. Lei, *Adv. Mater*., 2005, **17**, 1001.
13 F. Hu, Z. Li, C. Tu and M. Gao, *J. Colloid Interface Sci*., 2007, **311**, 469.
14 F. Hu, L. Wei, Z. Zhou, Y. Ran, Z. Li and M. Gao, *Adv. Mater*., 2006, **18**, 2553.
15 J.-H. Lee, Y. M. Huh, Y. Jun, J. Seo, J. Jang, H. T. Song, S. Kim, E.-J. Cho, H. G. Yoon, J. S. Suh and J. Cheon, *Nat. Med*., 2007, **13**, 95.
16 A. R. West, *Basic Solid State Chemistry*, Wiley, New York, 1988.
17 P. Saravanan, S. Alam, L. D. Kandpal and G. N. Mathur, *J. Mater. Sci. Lett*., 2002, **21**, 1135.
18 R. Schneider, F. Schmitt, C. Frochot, Y. Fort, N. Lourette, F. Guillemin, J.-F. Müllerd and M. Barberi-Heyob, *Bioorg. Med. Chem*., 2005, **13**, 2799.
19 S. Mohapatra, S. K. Mallick, T. K. Maiti, S. K. Ghosh and P. Pramanik, *Nanotechnology*, 2007, **18**, 385102.
20 K. L. Ang, S. Venkatraman and R. V. Ramanujan, *Mater. Sci. Eng., C*, 2007, **27**, 347.
21 J. S. Corneille, J.-W. He and D. W. Goodman, *Surf. Sci*., 1995, **338**, 211.
22 T. Schedel-Niedrig, W. Weiss and R. Schlogl, *Phys. Rev. B: Condens. Matter*, 1995, **52**, 17449.
23 A. Murza, S. Sánchez-Cortés, J. V. García-Ramos, J. M. Guisan, C. Alfonso and G. Rivas, *Biochemistry*, 2000, **39**, 10557.
24 S. Herrwerth, T. Rosendahl, C. Feng, J. Fick, W. Eck, M. Himmelhaus, R. Dahint and M. Grunze, *Langmuir*, 2003, **19**, 1880.
25 Y. Zhang, N. Kohler and M. Zhang, *Biomaterials*, 2002, **23**, 1553.
26 J. Zhang, S. Rana, R. S. Srivastava and R. D. K. Misra, *Acta Biomater*., 2008, **4**, 40.
27 Manasmita Das, Debasish Mishra, T. K. Maiti, A. Basak and P. Pramanik, *Nanotechnology*, 2008, **19**, 415101.
28 B. D. Cullity, *Introduction to Magnetic Materials*, Addison-Wesley, Reading, MA, 1972.
29 T. Mosmann, *J. Immunol. Methods*, 1993, **95**, 55.

